



Review

Introduction to super-resolution microscopy

Masahito Yamanaka^{1,2}, Nicholas I. Smith^{1,2}, and Katsumasa Fujita^{1,2,*}

¹Department of Applied Physics, and ²Immunology Frontier Research Center, Osaka University, Suita, Osaka, Japan

*To whom correspondence should be addressed. E-mail: fujita@ap.eng.osaka-u.ac.jp

Received 19 November 2013; Accepted 26 February 2014

Abstract

In this review, we introduce the principles of spatial resolution improvement in super-resolution microscopies that were recently developed. These super-resolution techniques utilize the interaction of light and fluorescent probes in order to break the diffraction barrier that limits spatial resolution. The imaging property of each super-resolution technique is also compared with the corresponding conventional one. Typical applications of the super-resolution techniques in biological research are also introduced.

Key words: Super-resolution microscopy, STED, PALM, STORM, SIM, SAX

Introduction

Optical microscopy has played a key role in biological and medical fields since optical microscopy allows us to image and investigate microorganisms, cells, tissues and organs in living conditions. With the aid of suitable fluorescent probes, microscopic images provide not only the structural information of the samples, but also a variety of information from the cellular environment, such as ion concentrations, membrane potential and signaling molecules. The non-invasiveness and the range of available imaging modalities have attracted researchers in biology, medicine and related research fields.

Although optical microscopy provides many different approaches to visualize various aspects of biological structures and activities, the spatial resolution of classical optical microscopes has been limited to approximately half the wavelength of the light used to probe the sample. The limitation in the spatial resolution stems from the wave nature of light and diffraction. Since the light propagates as an electromagnetic wave, it cannot be focused to an area smaller than the half of the light wavelength, as shown in Fig. 1, which directly determines the size of resolvable sample

structures. Due to the limitation on spatial resolution, referred to as ‘the diffraction limit’, biological interactions in the submicron scale environment were largely conjectured without imaging evidence.

In this review, we introduce the recent development of optical microscopy that has achieved spatial resolution beyond the diffraction limit. Intuitively, many biological events take place in a region smaller than the diffraction limit. These super-resolution microscopy techniques allow visualization to elucidate biological functions and phenomena, which in reality occur as an ensemble of biological events starting from the molecular scale. In the new microscopy concepts developed to achieve spatial resolution beyond the diffraction barrier, the key point is to exploit photo-switching of fluorescent probes or a non-linear response in the fluorescence emission. The primary way to realize such phenomena is the use of stimulated emission, photoactivation, *cis-trans* isomerization, triplet pumping and saturated excitation (SAX) (Table 1). So far, nearly all of the super-resolution microscopy implementations utilize the excitation and emission properties of fluorescent probes to break the diffraction barrier. Therefore, the current super-resolution

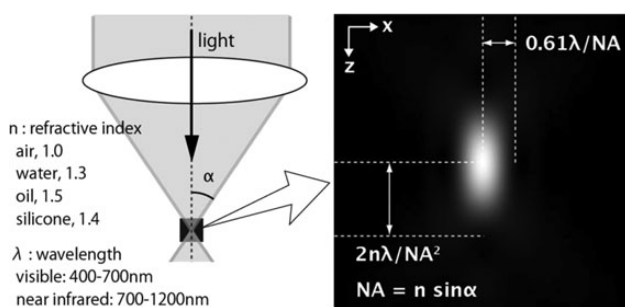


Fig. 1. Light distribution for focused light.

microscopes primarily target fluorescence-labeled samples. However, since fluorescence labeling is often a key element in biological imaging, the requirement of labeling for super-resolution is not a significant disadvantage.

In the latter sections, we describe the concept and properties of the super-resolution microscopes. We start from introducing the basics of image formation in optical microscopy to clarify the physics-based limitations on the spatial resolution, which helps readers to understand the concept of the super-resolution techniques. After this introduction, we describe the principles of several types of super-resolution microscopes and their imaging properties and applications. At the end of the article, we also discuss perspectives about the future development of super-resolution microscopes and related techniques. Since most super-resolution microscopes are developed for observation of fluorescent samples, we limit the description below to within the modality of fluorescence imaging.

Image formation in fluorescence microscopy

There are two types of fluorescence microscopy that are widespread in current experimental research. One is the ‘wide-field’ implementation and the other is laser scanning microscopy. These two techniques have different optical configurations and the mechanism of image construction is different; however, the spatial resolution limits are similar for both.

Figure 2a shows the image formation in wide-field fluorescence microscopy. The optical systems shown in Fig. 2 are schematic, but sufficient to show the limitation in the spatial resolution. In wide-field fluorescence microscopy, a sample is illuminated with light distributed uniformly across the field of view. Fluorescent probes, such as fluorescent molecules or quantum dots, are excited by the illumination light and fluorescence is emitted from each probe as it transitions to the ground state. Fluorescence is collected by an objective lens, and each fluorescent probe is imaged onto a detector, which is usually based on camera sensor elements such as CCD or CMOS, where it forms a fluorescence spot. Due to

the wave nature of light, the size of the fluorescence spot cannot be smaller than the diffraction limit and the image of fluorescent probes is blurred and individual probe spots overlap and cannot be resolved. This overlap of fluorescence spots then limits the resolvable size of the sample structure (or distribution of fluorescent probes) in wide-field fluorescence microscopy.

The image formation mechanism in laser scanning microscopy is slightly different from that of wide-field microscopy, but the limitation of the spatial resolution again arises from the wave nature. As shown in Fig. 2b, fluorescence molecules in a sample are excited by a laser focus. Fluorescence from the molecules is detected by a photodetector, and the laser focus is scanned over the sample to measure the fluorescence intensity at each position in the sample. A fluorescence image is then constructed as a spatial distribution of fluorescence signals detected at each point in the scan. The spatial resolution is restricted by the size of the excitation focus, and due to the wave nature of light, the spot size is limited to the half of the excitation wavelength. Therefore, multiple probes within the excitation spot cannot be separated by the laser scanning system. In confocal microscopy, the size of fluorescence spot at the pinhole, which is determined by wavelength of the fluorescence, also affects to the spatial resolution.

In both imaging systems, the spatial resolution is defined as the distance between two small fluorescence emitters that can be separately resolved. Since the image formation mechanisms are different in wide-field and laser scanning microscopies, the approaches to achieve spatial resolution beyond the diffraction limit are different for different microscopy implementations, as we demonstrate in the following sections.

Localization microscopy

As shown in Fig. 2a, the main reason for the limitation of spatial resolution in wide-field microscopy is the overlap of the fluorescence spots on the camera. This is inevitable when we try to record the fluorescence from each probe at the same time (Fig. 3a). However, what if we were to stop doing this and instead try to image fluorescent probes one by one? This is actually the main approach to realize super-resolution in wide-field microscopy.

It is difficult to separate fluorescent probes once they are imaged and overlapped since the overlap of many fluorescence spots cannot be unmixed. However, if only one fluorescent probe is imaged at a time, the position of the fluorescent probe can be isolated to a region much smaller than the fluorescence spot. Indeed, it can actually be determined with nanometer-scale accuracy [1]. As shown in Fig. 3b, the fluorescent molecules should be located at the

Table 1. Super-resolution fluorescence microscopy

Name	PALM/FPALM/STORM/GSDIM	SSIM	SIM	STED	RESOLFT	SAX
Key element to achieve super-resolution	Photoactivation, <i>cis-trans</i> isomerization, triplet pumping, etc.	Structured illumination + saturated excitation	Structured illumination	Stimulated emission	Photoactivation, <i>cis-trans</i> isomerization	Saturated excitation
Microscope type	Wide-field	Wide-field	Wide-field	Laser scanning	Laser scanning	Laser scanning
The number of required excitation light wavelengths	1–2	1	1	2	2	1
Spatial resolution						
Lateral	10–30 nm	~50 nm	100–130 nm	20–70 nm	40–80 nm	~120 nm
Axial	10–75 nm	Not reported	~300 nm	40–150 nm	Not reported	~300 nm
	Using opposing lenses, optical astigmatism, dual focus imaging or double-helical PSF			Using two opposing lenses or <i>z</i> -phase mask		
Z-stack range	Few hundreds nm–few μ m	Not reported	~Few μ m	~20 μ m	Not reported	30–50 μ m
Frame rate	s–min	s–min	ms–s	ms–s	s–min	s–min
Applicable fluorescent probe	Photoswitchable fluorescent proteins/molecules	Any if photostable	Any if photostable	Any if photostable	Photoswitchable fluorescent proteins	Any if photostable
Photodamage	Low–moderate	High	Moderate	Moderate–high	Low	Moderate–high
Photobleaching	Low	High	Moderate–high	Moderate–high	Moderate	Moderate–high
Required post-image processing	Yes	Yes	Yes	No	No	No

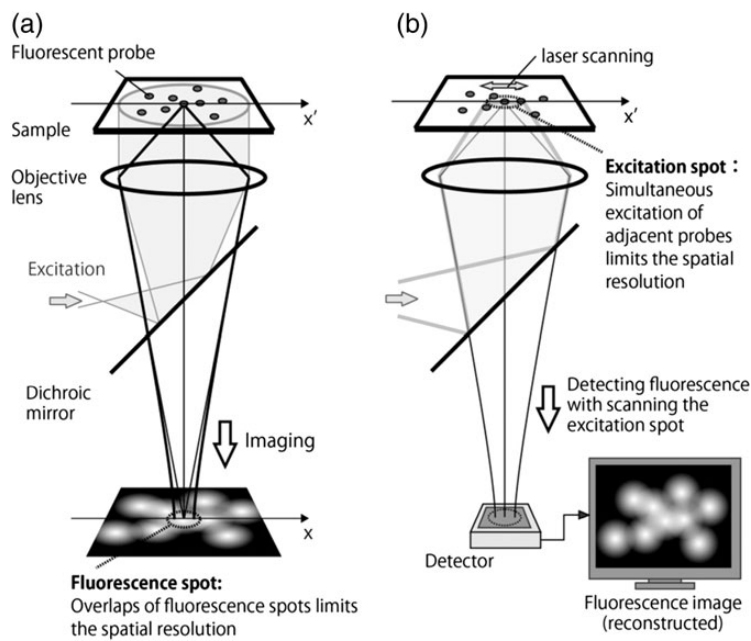


Fig. 2. Image formation in (a) wide-field and (b) laser scanning fluorescence microscopy.

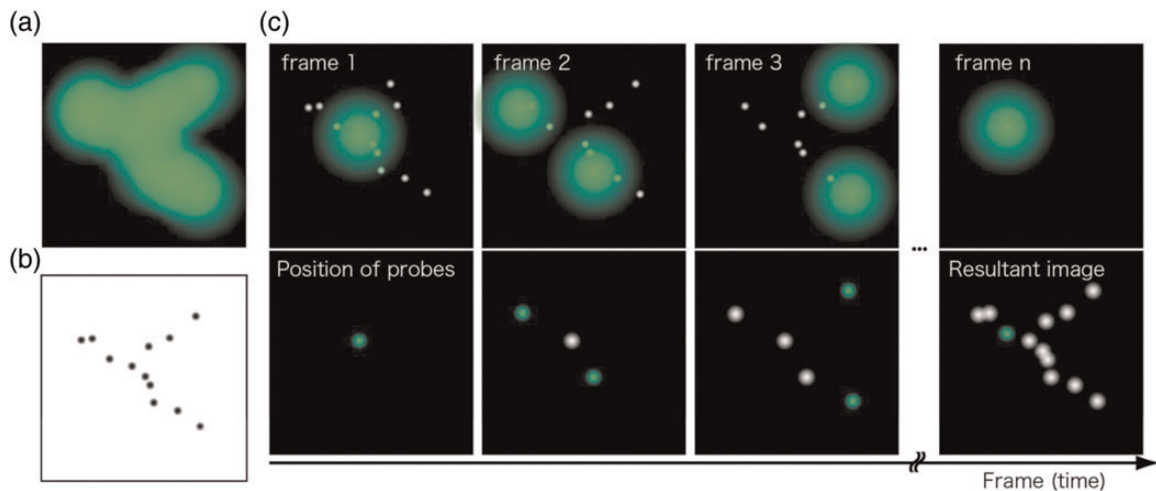


Fig. 3. (a) Fluorescence image obtained by conventional wide-field microscopy. All probes are imaged at a time and overlapped. (b) Distribution of fluorescent probes in a sample. (c) Image recording and construction in localization microscopy.

center of the fluorescence spot, and the position is determined by fitting a 2D Gaussian profile to the image or by centroid calculation [2]. Performing this single molecule localization for all fluorescent molecules in a sample provides a highly accurate map of the positions of fluorescent molecules in the sample, which is actually the fluorescence image with high resolution that we aim to obtain.

The issue in performing this localization approach is how to separate the emission of each molecule in a sample. In the proposed techniques, photoswitchable fluorescent probes are used to realize the concept. Photoswitchable

fluorescent probes change their emission wavelength or alternatively change the properties of light absorption or emission by light irradiation of a particular wavelength. Those probes can be turned 'off' so that they cannot be detected by the camera and can also be turned 'on' when we need to image them. To perform super-resolution imaging, a sample is stained with photoswitchable probes and they are turned 'off' initially. With weak irradiation of turning-'on' light to the sample, only a limited number of fluorescent probes are turned 'on' to be imaged by a conventional wide-field microscope, and then turned 'off' again for

the measurement of other probes. After recording the multiple images, each containing emission from only a fraction of the fluorescent probes, the data are processed and combined to construct a super-resolution image.

These localization-based super-resolution techniques were introduced by three different groups in 2006. These microscopes are termed photoactivation localization microscopy (PALM) [3], fluorescence photoactivation localization microscopy (FPALM) [4] and stochastic optical reconstruction microscopy (STORM) [5]. PALM and FPALM demonstrated the concept by using a photoactivatable fluorescent protein, PA-FP. STORM was demonstrated using a pair of synthetic dyes, such as Cy3–Cy5, that exhibits a switching property when the fluorophores are closely located [6]. In the three named implementations mentioned above, although the fluorescent probes and the technical details are different, the principle for constructing a super-resolution image is the same. Therefore, these techniques can be categorized as ‘localization microscopy’ from the concept of image construction. Figure 4 shows a comparison of fluorescence images of mitochondria (magenta) and microtubules (green) observed by (Fig. 4a) conventional wide-field microscopy and (Fig. 4b) STORM. The spatial resolution is notably improved in the STORM image.

The key of the localization approach is switching fluorescent probes between ‘on’ and ‘off’ states. After the introduction of PALM/FPALM/STORM, several different approaches for switching the state of fluorescent probes are proposed. It has been reported that even a single fluorophore can exhibit the switching capability [7]. This approach is called dSTORM (direct STORM) and has reduced the limitation on the available fluorescent probes that can be used for localization microscopy [8, 9]. An imaging technique called GSDIM (ground state depletion followed by individual molecule return) turns off fluorescent probes by forcing the probe transition to a long-lived ‘off’ state, which is the triplet or unknown dark state, by repeated light excitation [10]. The technique exploits the spontaneous recovery to the excitable ground state for turning the probes on. Therefore, GSDIM

does not require switching light sources for control of the probe state, so a simple wide-field fluorescence microscope equipped with a high power excitation source can realize super-resolution imaging. This switching-free approach has also been demonstrated by using fluorophores where the lifetime of the non-fluorescent state was lengthened by reduction in the triplet state to a radical anion [11]. The shift of the emission spectrum of quantum dots has also been utilized to control the ‘off’ time, allowing the use of bright emission from quantum dots for improving the localization accuracy [12].

The spatial resolution of localization microscopy is determined by the precision of the localization. In 2D Gaussian fitting, the precision is given as σ/\sqrt{N} , where σ is the standard deviation of the single probe measurement, which corresponds to the point spread function of the optics (PSF), and N is the number of photons. Assuming a Gaussian distribution, the spatial resolution is given as $2.35 \times$ the localization precision (FWHM of the Gaussian). The spatial resolution can be improved by increasing the number of photons detected from each probe and is no longer limited by the diffraction. A spatial resolution of 6 nm was demonstrated by using bright photoactivatable dyes created by reductive caging in STORM [13]. However, some research groups reported that the precision of the localization is affected by the molecular orientation and the rotation motility of fluorescent probes [14, 15]. The position-dependent aberration also can cause artifacts in the image [16]. These issues would be the next barrier to achieve the ultimate spatial resolution using the localization approach.

The localization can also be performed in three dimensions (3D). For 3D localization imaging, the imaging optics has to be modified to obtain the information of axial displacement of fluorescent probes. 3D-STORM inserts a cylindrical lens between the objective and tube lens to introduce astigmatism in the imaging system. The z position of the probe can then be measured as elliptical deformation of the fluorescence spot on a camera [17]. The dual-focus imaging technique with a single objective lens and a camera has also been used for 3D localization imaging [18]. It is also possible to use a double helical point spread function to encode the z position, which grants a wider axial range of localization than the astigmatism and dual-focus methods [19, 20]. The use of two opposing objective lenses for more accurate z -position measurement has also been introduced in different implementations [21–23].

Since localization microscopy requires multiple single molecule images for constructing a super-resolution image, its temporal resolution is typically low. The number of frames required to image construction increases with an increase in the number of probes in a field of view. A straightforward way to improve the temporal resolution is the increase in the frame rate of image acquisition. By using

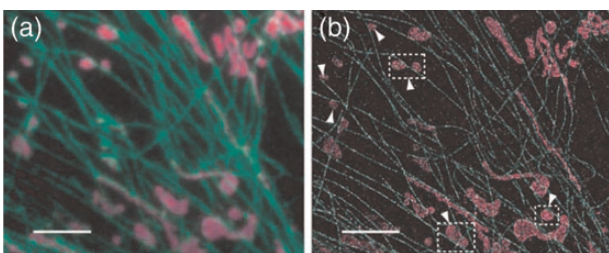


Fig. 4. Fluorescence images of mitochondria (magenta) and microtubules (green) observed by (a) conventional wide-field microscopy and (b) STORM. Scale bar = 3 μ m. Reprinted by permission from Macmillan Publishers Ltd: Nat. Methods (doi:10.1038/nmeth.1274).

high-quantum-efficiency and high-speed sCMOS cameras, 2–32 frames/s frame rate has been achieved [24, 25]. Another approach for fast image acquisition is increasing the number of fluorescent probes that can be imaged in the same camera frame. For this approach, algorithms that localize individual molecules even from overlaps of several fluorescence spots have been proposed [26, 27]. The use of compressed sensing has also been introduced and allowed the localization of molecules at the concentration of 8 molecules/ μm^2 in an image, which is about eight times higher than that in typical localization microscopy [28]. Bayesian statistics has also been applied to localized individual molecules in a series of fluorescence images with highly overlapped fluorescence spots by considering the characteristics of blinking and photobleaching of the molecules [29]. SOFI (super-resolution optical fluctuation imaging) also utilizes the temporal fluctuation to improve the spatial resolution [30, 31]; however, it does not construct a fluorescence image by localization of molecules.

Localization microscopy is especially useful to observe ultra-fine structures in a cell. For high accuracy localization, STORM using synthetic probes has an advantage in the number of choices of fluorescent probes for the technique [32]. A combination with Halo/SNAP tags and equivalent techniques allow us to apply the synthetic dyes for live cell STORM imaging [33]. STORM has been used to reveal intracellular structures, such as actin and spectrin architecture in axons [34]. Dynamics of plasma membrane, mitochondria, endoplasmic reticulum or lysosomes were also observed by photoswitchable membrane probes [35]. The technique has also been applied to image protein distributions in a body or biofilm assembly of microbes [36]. PALM is inherently suited to observe living samples since it utilizes the photoswitchable fluorescent proteins synthesized in a

cell, and for example, observations of cell adhesion and bacterial actin protein in live cells were demonstrated [37, 38]. PALM also has been applied to image and count molecules in single organelles in yeasts, which can be an important approach to quantitatively understand biological functions in the molecular scale. PALM is especially advantageous in observation of structures in specimens where synthetic probes are difficult to use, such as tissues, and time-lapse observation of cell functions and developments.

Localization microscopy has typically been applied to the observations of thin samples or for a sample surface since it is difficult to achieve a high localization accuracy in imaging a deep path of a sample. So far, the use of two-photon excitation and selective plane illumination has been examined to realize super-resolution imaging of thick samples [39, 40].

Structured illumination microscopy

Structured illumination microscopy (SIM) is also one of the super-resolution techniques using the wide-field configuration. SIM does not require a special fluorescent probe for the resolution improvement, but takes a more optical approach to bring out the full potential of wide-field fluorescence microscopy.

The difference between SIM and the conventional fluorescence microscope is the illumination pattern on a sample [41]. SIM illuminates a sample with a light distribution like a grid as shown in Fig. 5b, resulting in moiré fringes in the emission distribution. This moiré keeps the information of the small structure in the sample even after the blurring effect during image formation in the optics. Since the position and the period of the illumination grid is already known, we can recover information of the fine structure

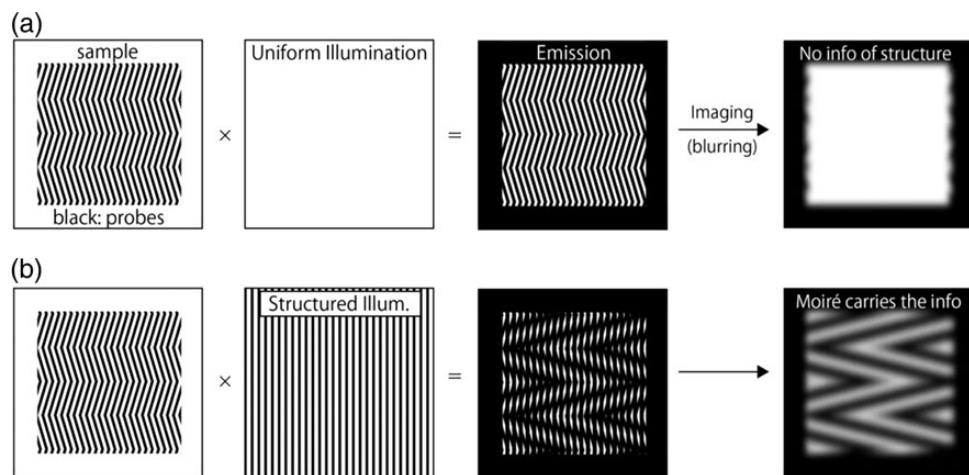


Fig. 5. A comparison of image formation between (a) conventional wide-field and (b) structured illumination microscopy.

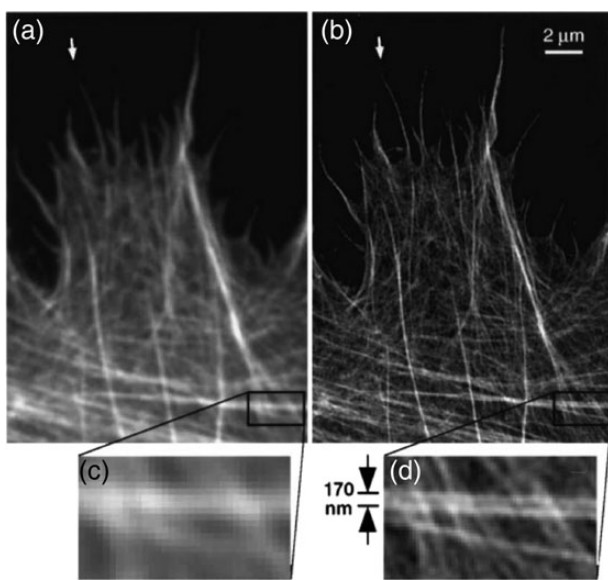


Fig. 6. Actin cytoskeleton observed by (a) conventional wide-field and (b) structured illumination microscopy. Reprinted from Ref. [41] by permission from John Wiley and Sons.

obtained as the moiré. Whereas, in conventional fluorescence microscopy, the fine structures cannot be recovered because they are fundamentally missing from the imaging process (Fig. 5a). Figure 6 shows images of actin cytoskeleton observed by (Fig. 6a) conventional wide-field and (Fig. 6b) SIM. The clear improvement of the spatial resolution is confirmed in the SIM image. The concept of super-resolution imaging with structured illumination was first introduced by Lukosz [42] for bright-field microscopy and later successfully implemented in fluorescence microscopy [41]. A similar approach was also taken for achieving z-resolution in wide-field imaging [43].

The improvement of the spatial resolution in SIM can be understood more clearly using simple mathematics. Figure 7 shows the mathematical view of image formation in conventional fluorescence microscopy and SIM. In fluorescence microscopy, a fluorescence image of a sample is given as the convolution of the emission pattern from the sample, which is the distribution of fluorescent probes, and the point spread function of the imaging optics. This process

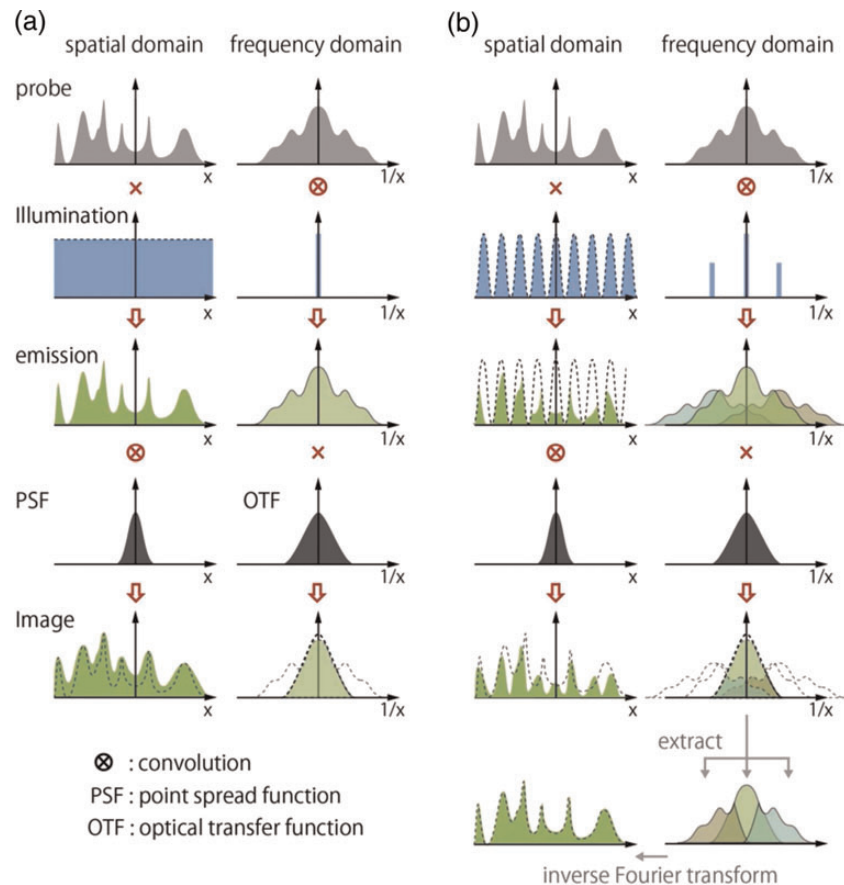


Fig. 7. Image formation in (a) conventional wide-field and (b) structured illumination microscopy. In structured illumination microscopy, high-frequency components in the sample can be imaged due to the frequency shift by the structured illumination; however, they are overlapped with lower frequency image components. Three overlapped components are extracted and reconstructed in the frequency domain. The inverse Fourier transform allows reconstruction of a fluorescence image with high spatial-frequency information.

corresponds to applying a low spatial-frequency pass filter to the emission distribution as seen in Fig. 7a (frequency domain). In conventional fluorescence microscopy, the high spatial-frequency components, which represent small structures in the sample, are cutoff by the low-pass filtering and cannot be recovered even by post-processing of the image. On the other hand, in SIM, the high spatial-frequency components still remain in the resultant images because the grid illumination shifts the high spatial-frequency components near to the DC frequency, allowing them to pass through the low-pass filter inherent in the image formation. This frequency shift is seen as the moiré, in which the high- and low-frequency components are overlapped as seen in Fig. 7b (frequency domain). These overlapped frequency components have to be extracted to make the fine structure recognizable in the fluorescence image (Fig. 7b bottom-right). To extract the overlapped components, three fluorescence images are obtained with the structured illuminations with three different phases.

The spatial resolution in SIM is improved by a factor of 2 from conventional microscopy. As shown in Fig. 7b, the convolution of the frequencies from the illumination pattern and the sample is responsible for the shift of high-frequency components to lower frequencies that can be imaged through the low-pass filter. A finer illumination grid creates higher resolution. However, since the illumination pattern itself is produced by the objective lens, the periodicity of the grid pattern is also limited by diffraction. Therefore, the finest grid corresponds to the smallest structure resolvable by conventional microscopy, and the maximum frequency shift is located at the edge of the low-pass filter. Under these conditions, the amount of the frequency shift corresponds to the bandwidth of the imaging system in conventional microscopy, and the improvement of the resolution is hence a factor of 2.

Confocal fluorescence microscopy also has twice higher spatial resolution compared with conventional microscopy, if compared strictly by limiting frequencies in the frequency domain [44]. However, SIM exhibits the greater image contrast of small structures than confocal microscopy. This is because contrast is not simply a function of maximum frequency, and the illumination in confocal microscopy has more low-frequency components than SIM, resulting in the low-frequency-enhanced contrast. Since the dynamic range of fluorescence detection is severely limited by the number of fluorescence photons from a sample and also by the detection noise, this low-frequency enhancement property of confocal microscopy is disadvantageous in imaging sample structures with spatial frequencies close to the cut-off. On the other hand, the illumination in SIM has much less low-frequency components in the illumination,

allowing us to use the full spatial-frequency bandwidth of the microscope to image small structures.

The above discussion describes how the spatial resolution of SIM is still determined within the regime of diffraction. For improving the resolution further, exploiting fluorescence emission driven non-linearly by the excitation intensity has been examined. Saturated structured illumination microscopy (SSIM) expands the resolving power of SIM to the regime beyond the diffraction limit [45, 46]. In SSIM, the sample is excited by the same illumination pattern to that in SIM; however, the fluorescence excitation is saturated by high excitation intensity. With SAX, the pattern of fluorescence emission on the sample is distorted from that of the illumination and then possesses additional harmonic frequency components. The harmonic frequencies appear at a higher frequency region that is actually outside of the illumination band frequencies. The harmonic frequency components in the emission pattern shift the higher frequency components of the sample structure into the detectable frequency that can be imaged, and can then be extracted by image processing similar to SIM.

SSIM was demonstrated in the observation of fluorescent beads and clearly resolved the 40 nm diameter beads with excitation by a nanosecond pulsed laser. Since the SAX in wide-field microscopy requires high laser power, this technique was believed to be not applicable to biological samples. However, recently, this problem was overcome by using photoswitchable fluorescent probes. By applying a structured illumination for switching, a ‘structured’ emission capability, which corresponds to the patterned emission in SIM, can be formed in a sample. Since photoswitchable probes retain their on/off state for a relatively long period, long exposure to the switching light cause a distortion in the ‘structured’ emission capability, allowing us to exploit the high harmonic frequency which appears in the emission pattern to resolve the smaller structures. By using this technique, 50 nm lateral resolution has been achieved in imaging of actin cytoskeleton and nuclear pores in a fixed cell [47].

The concept of SIM is also applied in 3D. One of the major approaches is a method using three-beam interference to extend the 2D illumination pattern to 3D [48]. By obtaining a z-stack of $x-y$ images and computational processing, the 3D SIM achieves a single 3D image with ~ 100 nm lateral and ~ 300 nm axial resolution. Another well-known approach is based on a side illumination scheme utilizing light sheet or Bessel beam illumination [49]. In the light sheet illumination scheme, the structured illumination pattern is created by the combination of laser scanning and temporal modulation of the laser intensity. On the other hand, in the Bessel beam illumination approach, the laser beam irradiates the sample at discrete and periodic points at

a given period along the beam scanning direction to produce a structured illumination pattern. These side illumination methods offer fast 3D imaging capability with high spatial resolution and image contrast.

The image acquisition speed in SIM has been improved recently by implementing a liquid crystal spatial light modulator to allow quick switching of the illumination orientation and phase. This technique pushes the image acquisition speed up to \sim 11 Hz [50]. Time-lapse SIM observations of cellular organelles and cytoskeletons, such as microtubules, mitochondria and actin filaments, were used to demonstrate the technique [51, 52].

SIM has been already applied in some biological studies. Using multicolor 3D SIM, the structures of chromatin and colocalization of single nuclear pore complexes and nuclear lamins in a mammalian cell were observed [53]. Investigations of immune synapses in natural killer cell [54], intermediate states of abscission in human cells [55] and pericentriolar material in the centrosome [56, 57] were also performed. Recently, time-lapse studies of 3D dynamics in living specimens with Bessel beam structured illumination was also reported [58].

STED/RESOLFT/GSD microscopy

As shown in Fig. 2b, the spatial resolution of laser scanning microscopy is limited by the spot size of laser illumination. The spot size is strictly limited by the wave nature of light, and the light cannot be focused into an area smaller than the half of the wavelength. Using laser light with a shorter wavelength helps us to make the illumination spot smaller; however, for observation of biological samples, it is nearly

always preferable to use visible or near-infrared (NIR) light to avoid sample damage.

Since it is difficult to reduce the physical size of the focused laser spot, most super-resolution techniques in laser scanning microscopy try to limit the region of fluorescence detection to an area smaller than the diffraction-limited spot; this is governed by different physics and can be changed independently of the spot size.

The technique of stimulated emission depletion (STED) microscopy utilizes stimulated emission to restrict the fluorescence emission to within a small area inside the larger excitation laser spot. As shown in Fig. 8a, STED microscopy excites the fluorescent probes in the sample with focused laser light. The sample is also illuminated by an STED beam (i.e. depletion beam) that suppresses the spontaneous emission by inducing stimulated emission from the excited molecules. The STED beam is formed in a donut-like focus shape that has zero light intensity at the center of the excitation spot so that only the center of the excitation focus is allowed to emit fluorescence spontaneously. By filtering out the stimulated emission and the STED beam using a wavelength filter, we can detect only the spontaneous emission that is localized within the center area of the excitation spot. By scanning the excitation and STED beam together in the sample and measuring the intensity of spontaneous emission, the distribution of fluorescent probes in the sample can be recorded with a spatial resolution higher than when scanning without using the STED beam. Figure 9 shows fluorescence images of neurofilaments in human neuroblastoma observed by (Fig. 9a) confocal and (Fig. 9b) STED microscopy. By the incidence of the STED beam, the spatial resolution was improved, and small structures, that were not

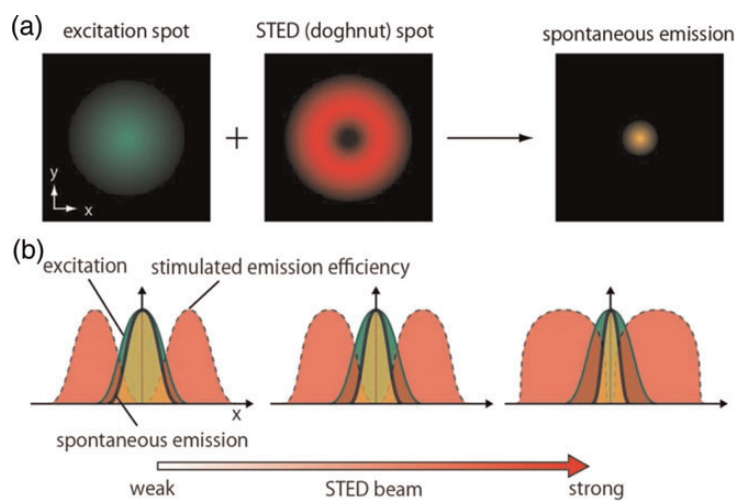


Fig. 8. (a) Principle of the resolution improvement in STED microscopy. (b) Saturation effect in stimulated emission reduces the region for spontaneous emission.

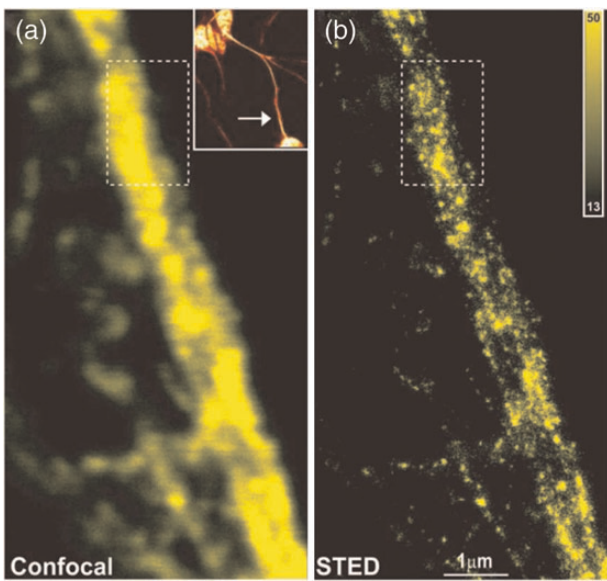


Fig. 9. Neurofilaments in human neuroblastoma observed by (a) confocal and (b) STED microscopy. Reprinted from Ref. [59]. Copyright (2006) National Academy of Sciences, USA.

recognizable in the confocal image, can be clearly observed in the STED image.

The spatial resolution of STED microscopy is determined by the size of the area where the spontaneous emission is allowed, which is primarily determined by the size of the donut hole of the STED beam. The donut hole is produced by interference of light waves; therefore, similar to limitations described above, its size cannot be smaller than the half the STED beam wavelength, and the corresponding spatial resolution is equivalent to that of confocal microscopy. However, in STED microscopy, there is another trick to break the diffraction barrier.

STED microscopy utilizes the saturation of stimulated emission to reduce the area of spontaneous emission further. The size of the donut hole in the focused STED beam cannot be smaller than half of the light wavelength, but the size of the hole in the region of stimulated emission can be smaller. As shown in Fig. 8b, the area that shows spontaneous emission can be reduced by increasing the intensity of the STED beam, because the efficiency of stimulated emission cannot exceed 100%. With the increase in the intensity of the STED beam, the area showing stimulated emission increases, and spontaneous emission is restricted to a smaller and smaller area. This is because, for the relevant intensities used here, the center of the donut retains zero stimulated emission, regardless of the intensity of the STED beam. The spatial resolution is then determined by the intensity of the STED beam, and it is practically limited by photobleaching of the fluorescent probes, which can occur after repeated excitation and stimulated emission. Typically, 20–70 nm spatial resolutions can be

demonstrated in imaging biological samples stained with synthetic dyes and fluorescent proteins. A much higher spatial resolution of 6 nm has also been demonstrated in observation of nitrogen-vacancy color centers in diamond that show extremely high photostability [60]. The spatial resolution can also be improved in the z -direction by controlling the STED beam shape. By introducing two STED beams, each for improving xy and z resolutions, at the same time, an isotropic 3D resolution can be realized [61].

The image acquisition time of STED microscopy depends on the number of scanning points. Video-rate imaging of synaptic vesicles in a neuronal axon was performed with a 62 nm spatial resolution [62]. Using multiple foci for scanning has also a potential to improve the spatial resolution further [63]. Compared with wide-field super-resolution microscopy, the characteristics of the motion artifacts appear different in STED microscopy. Artifacts in a local area in an STED image can be smaller since the time difference of fluorescence measurement across the image is constant and smaller in STED microscopy compared with wide-field counterparts that stochastically image fluorescent probes in a view area.

In live cell or tissue imaging, the high intensity of the STED beam may cause photodamage to the sample, which makes it difficult to perform time-lapse observation of biological activities. STED microscopy requires a high-intensity STED beam because the lifetime of the excitation state of the fluorescent probe can be several nanoseconds, and the depletion by stimulated emission has to be performed within this lifetime, which requires irradiation of a high density of photons. Therefore, the early demonstrations of STED microscopy were performed with a pulsed laser [59]. Later, a CW laser was also applied for STED, with the possibility of reducing photodamage which arises non-linearly with the beam intensity [64]. Using a CW laser also has reduced the requirements of the components in STED microscopy; however, the efficiency of stimulated emission is lower compared with pulsed STED microscopy. This disadvantage was overcome by using gated detection of the spontaneous emission [65].

For reducing the STED beam intensity further, a technique called RESOLFT (reversible saturable optical fluorescence transitions) is effective. RESOLFT utilizes switchable fluorescent probes to confine the detectable fluorescent probes within the focal volume by turning off the probes by the donut beam. Since the on/off state of switchable probes have much longer lifetime compare with that of the excitation state, the light intensity required to turn off the probes is much smaller than that in STED microscopy [66, 67]. GSD (ground state depletion) microscopy takes a similar approach to RESOLFT, but it exploits the triplet or dark state of fluorescent molecules [68, 69] that was also used

in GSDIM. Although RESOLFT/GSD reduce the beam intensity for controlling the fluorescence emission, the slow switching speed is actually disadvantageous in live cell imaging. To tackle this issue, a photoswitchable fluorescent protein, rsEGFP2, has been developed to increase the switching speed and applied to imaging the dynamics of endoplasmic reticulum with the temporal resolution of 0.5 s and the 9 μm^2 field of view [70]. The use of multiple donut beams was also proposed in RESOLFT microscopy, and an image acquisition time of 3 s for imaging a whole cell (120 $\mu\text{m} \times 100 \mu\text{m}$ field of view) with a spatial resolution <77 nm was demonstrated [71].

A wide range of biological studies using STED microscopy have already emerged. So far, a variety of intracellular architectures [i.e. endoplasmic reticulum (ER) and microtubules] have been visualized [72]. On the top of that, the details in such cellular organelles were also investigated. For examples, the distribution of protein Tom20 in mitochondria [61, 73], membrane microdomain formation and cytoskeleton structuring induced by interleukin-7 [74], and the colocalization of the subunits in nuclear pore complexes [75] were revealed. STED microscopy is also applied in neuronal biological investigations [76]. The observation of synaptic vesicles in a bouton of neurons revealed the behavior of synaptotagmin after exocytosis of synaptic vesicles [77]. Furthermore, the video-rate imaging capability of STED microscopy allows us to visualize the synapse vesicle movement [62]. Dendric structures in neuron were also visualized [78] and time-lapse STED imaging of dendric spines revealed that the morphological plasticity of dendritic spines is determined by the synaptic activity [79]. Recently, super-resolution imaging deep inside living brain slices was performed, and the dynamic organization of actin bundles inside synapses were investigated [80]. By applying STED microscopy concept to fluorescence correlation spectroscopy (STED-FCS), it is also feasible to study molecular dynamics in nanoscale regions. The nanoscale dynamics of diffusing lipid molecules, such as phosphoglycerolipids and phosphoglycerolipids, in a living cell plasma membrane was revealed with STED-FCS [81]. By using fluorescence recovery after photobleaching analysis with STED microscopy, the behaviors of membrane protein clusters were also clearly observed [82]. Furthermore, the combination of STED microscopy and optical tweezers techniques was recently demonstrated and has enabled studies of protein binding and dynamics on DNA under high concentration of proteins [83].

SAX microscopy

Another approach to achieve super-resolution in laser scanning microscopy is a method using SAX. SAX is induced due to non-zero fluorescence lifetime and the depletion of

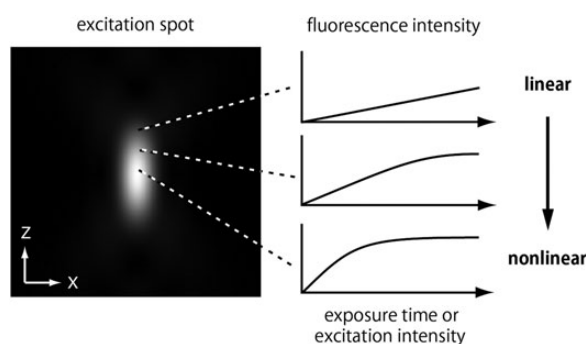


Fig. 10. Principle of the resolution enhancement in SAX microscopy. Extraction of fluorescence signals responding non-linearly to either the excitation or the exposure time allows the detection of fluorescent probes in an area smaller than the focal volume.

the population of the ground state mainly through a transition to the triplet state. Under the SAX condition, the fluorescence intensity becomes non-linearly proportional to the excitation intensity.

For the improvement of the spatial resolution, the non-linear fluorescence response induced by SAX is utilized to reduce the size of the fluorescence detection volume below the diffraction limit. When a laser light is focused into a sample, SAX predominantly occurs in the center of the laser focus spot where the excitation intensity is high (Fig. 10). Therefore, the detection of the SAX-induced non-linear signals allows us to detect fluorescence emission from only a small fraction within the focal spot, resulting in the spatial resolution enhancement, and this resolution improvement is inherently 3D.

The extraction of the non-linear signal is, however, not straightforward, because the linear signal still exists under the SAX condition. Several techniques for the extraction were reported so far. The time dependence of the fluorescence response was first utilized because the evolution of the saturation requires a certain time determined by the photophysical parameters of fluorescent molecules, such as fluorescence lifetime and triplet lifetime [84]. Temporal modulation of the excitation followed by harmonic demodulation of the fluorescence signal was also used for the extraction (referred as SAX microscopy) [85, 86]. Recently, the technique based on the measurement of fluorescence intensity dependence on the excitation at each observed position and subsequent curve fitting was demonstrated [87]. Among the proposed techniques, SAX microscopy is an approach that more easily turns conventional laser scanning confocal microscopy into super-resolution microscopy.

The improvement of the spatial resolution using SAX is theoretically unlimited. However, practically, the requirement of the high excitation intensity does limit the achievable spatial resolution because of photobleaching effects

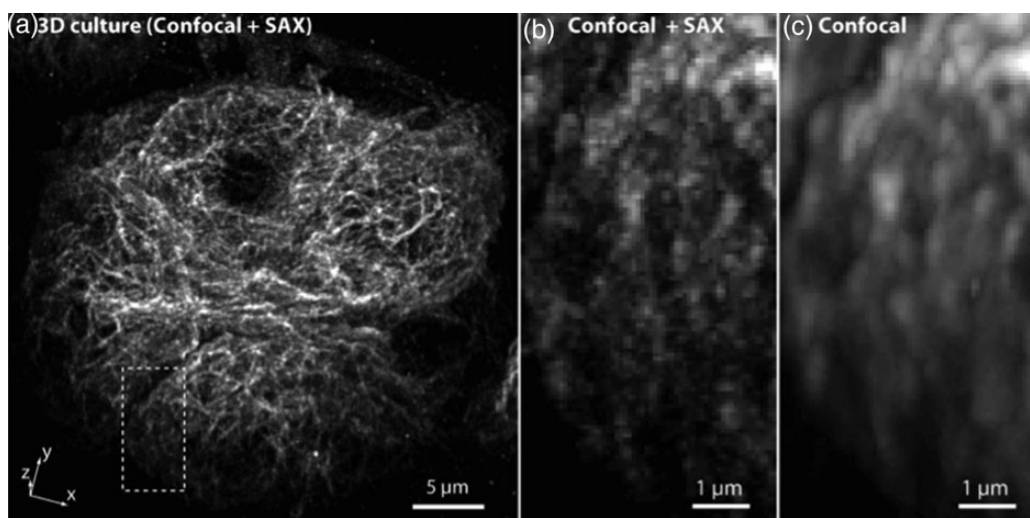


Fig. 11. 3D projection image of tubulin in HeLa cells cultured in 3D. (a) Whole cell cluster observed by confocal SAX. (b and c) Confocal SAX and confocal images of the dotted area in (a). Reprinted from Ref. [92].

and the resultant decrease in signal-to-noise ratio in fluorescence detection. In SAX microscopy, 1.4- to 2-fold higher spatial resolution in 3D than confocal microscopy was achieved in the observation of fluorescent nanodiamonds and also with biological samples stained with conventional organic dyes or fluorescent proteins [88–90]. The method based on curve fitting technique shows ~1.4-fold improvement of the spatial resolution in the *x*-*y* plane compared with confocal microscopy [87].

The non-linear nature of the fluorescence emission also allows us to improve the depth discrimination properties, in addition to the improvement of the spatial resolution. Since SAX is induced by high excitation intensity, the non-linear fluorescence signals are strongly localized in the laser focus. Therefore, the use of the non-linear signals enables the effective suppression of the detection of fluorescence signals from out-of-focus planes. The high background elimination property of SAX allows us to observe finer structures in a thick sample with high spatial resolution and imaging contrast [91, 92]. Figure 11 shows the result of volumetric imaging of α -tubulin in a cell cluster obtained with SAX microscopy. The magnification of the boxed area in Fig. 11a is shown in Fig. 11b. For comparison, the same area was observed with confocal mode (Fig. 11c). The comparison clearly shows significant improvement of the image contrast by the SAX mode, and the improvement allows us to observe more detailed structures in the sample.

Outlooks

As introduced above, several types of super-resolution microscopy have been proposed and developed. Localization microscopy, STED-type microscopy and SIM are

available in the market and have already been utilized in practical research fields. However, these super-resolution microscopes are still not applicable to many biological or medical applications. In practical usage, one has to understand the mechanism of the imaging property and the limitation of the technique. Thus, it is extremely important to analyze and interpret the obtained experimental data. This review cannot cover all aspects of the super-resolution techniques; however, there are many review articles and guidelines that introduce the techniques and applications from different points of view [93–96].

Although many types of super-resolution technique have been developed, there are still many issues in observation of living samples. The improved spatial resolution can show more details of the sample structure; however, the image is easily affected from the motion of the sample. To avoid deriving a wrong conclusion from such an image, the experimental conditions, such as the temporal and spatial resolutions, have to be carefully chosen. For instance, given the spatial resolution, the required temporal resolution can be estimated from the speed of the target structure in the sample. The labeling condition, especially the choice of probe and probe concentration, is also an important factor to image the sample structure properly [97]. In addition, photodamage presents a significant problem for many super-resolution techniques, since a great number of photons are often required to resolve structural details in the sample. In the case of localization-based techniques, to achieve ~6 nm spatial resolution, $\sim 10^5$ photons are required per ‘localization’, which does not alone give a super-resolved image, but is combined with a large number of images, each containing localization information from a fraction of the probes in the field of view to produce the

final image [13]. For the STED/RESOLFT approaches, a certain number of photons (for example, ~10–50 photons per pixels) are required to obtain an image with sufficient SN ratio for observations of the small details in sample structures. In order to detect 10–50 photons per pixel, the number of photons required to irradiate the sample will be orders of magnitude higher, depending on the probe used, the probe concentration, the sample conditions and the wavelengths of both beams. This photon requirement becomes more severe when faster image acquisition is required. Observation of a thick sample is also a challenge since aberration and light scattering in a sample make it difficult to perform the precise control of light propagation and act to decrease the signal-to-noise ratio of fluorescence measurement.

Naturally, the above issues are the next targets of the technology development that actually involves many different science and technology fields. One of the main issues is the photon budget. Since many techniques require numbers of photons to construct a high-resolution image, increasing the number of available photons from a probe is key. Recently, it was reported that reductive caging can be used to create bright photoswitching dyes and it increases the available number of photons more than 10 times in localization-based techniques [13]. The efficient use of photons (which is also helpful to reduce photodamage) is important to optimize to ensure sufficient imaging quality. With epi-illumination conditions, a huge number of emitted fluorescence photons are wasted because regions in out-of-focus planes are also exposed to excitation light illumination. The use of Bessel beam or light sheet illumination approaches allows us to illuminate only the observation area in a sample, and then helps to increase the number of photons for imaging and reduce the phototoxicity [49]. Applying adaptive optics and development of long-wavelength fluorescent probes would become more important for super-resolution imaging of thick samples. By using adaptive optics techniques with a spatial light modulator, it is feasible to correct aberrations induced by a sample. This technique enables 3D super-resolution imaging of thick specimens by STED microscopy [98]. The use of NIR wavelength for fluorescence excitation and detection also helps to improve the imaging depth because of the low light scattering and absorption efficiency in biological samples at this wavelength range [99]. Low light absorption characteristics of the sample are quite advantageous for live cell imaging.

There are also several attempts to expand the super-resolution techniques for imaging non-fluorescent samples. For instance, the use of saturable absorption or scattering has been demonstrated [100–102]. Super-resolution techniques using coherent Raman scattering and sum frequency generation were also proposed [103, 104], where molecular

vibrations are utilized to visualize sample structures without labeling. These techniques would compensate fluorescence techniques and make the role of optical microscopy more important in biological and medical research fields.

Funding

This study was supported by the Next Generation World-Leading Researchers (NEXT Program) of the Japan Society for the Promotion of Science (JSPS) and the Network Joint Research Center for Materials and Devices.

References

1. Gelles J, Schnapp B J, Sheetz M P (1988) Tracking kinesin-driven movements with nanometre-scale precision. *Nature* 331: 450–453.
2. Andersson S B (2008) Localization of a fluorescent source without numerical fitting. *Opt. Express* 16: 18714–18724.
3. Betzig E, Patterson G H, Sougrat R, et al. (2006) Imaging intracellular fluorescent proteins at nanometer resolution. *Science* 313: 1642–1645.
4. Hess S T, Girirajan T P K, Mason M D (2006) Ultra-high resolution imaging by fluorescence Photoactivation Localization Microscopy. *Biophys. J.* 91: 4258–4272.
5. Rust M J, Bates M, Zhuang X (2006) Sub-diffraction-limit imaging by stochastic optical reconstruction microscopy (STORM). *Nat. Methods* 3: 793–796.
6. Bates M, Blosser T, Zhuang X (2005) Short-range spectroscopic ruler based on a single-molecule optical switch. *Phys. Rev. Lett.* 94: 108101.
7. Heilemann M, Margeat E, Kasper R, et al. (2005) Carbocyanine dyes as efficient reversible single-molecule optical switch. *J. Am. Chem. Soc.* 127: 3801–3806.
8. Heilemann M, Van de Linde S, Schüttpelz M, et al. (2008) Subdiffraction-resolution fluorescence imaging with conventional fluorescent probes. *Angew. Chem. Int. Ed.* 47: 6172–6176.
9. Heilemann M, Van de Linde S, Mukherjee A, Sauer M (2009) Super-resolution imaging with small organic fluorophores. *Angew. Chem. Int. Ed.* 48: 6903–6908.
10. Fölling J, Bossi M, Bock H, et al. (2008) Fluorescence nanoscopy by ground-state depletion and single-molecule return. *Nat. Methods* 5: 943–945.
11. Steinhauer C, Forthmann C, Vogelsang J, Tinnefeld P (2008) Superresolution microscopy on the basis of engineered dark states. *J. Am. Chem. Soc.* 130: 16840–16841.
12. Hoyer P, Staudt T, Engelhardt J, Hell S W (2011) Quantum dot blueing and blinking enables fluorescence nanoscopy. *Nano Lett.* 11: 245–250.
13. Vaughan J C, Jia S, Zhuang X (2012) Ultrabright photoactivatable fluorophores created by reductive caging. *Nat. Methods* 9: 1181–1184.
14. Engelhardt J, Keller J, Hoyer P, et al. (2011) Molecular orientation affects localization accuracy in superresolution far-field fluorescence microscopy. *Nano Lett.* 11: 209–213.

15. Lew M D, Backlund M P, Moerner W E (2013) Rotational mobility of single molecules affects localization accuracy in super-resolution fluorescence microscopy. *Nano Lett.* 13: 3967–3972.
16. Quirin S, Pavani S R P, Piestun R (2012) Optimal 3D single-molecule localization for superresolution microscopy with aberrations and engineered point spread functions. *Proc. Natl Acad. Sci. USA* 109: 675–679.
17. Huang B, Wang W, Bates M, Zhuang X (2008) Three-dimensional super-resolution imaging by stochastic optical reconstruction microscopy. *Science* 319: 810–813.
18. Juette M F, Gould T J, Lessard M D, et al. (2008) Three-dimensional sub-100 nm resolution fluorescence microscopy of thick samples. *Nat. Methods* 5: 527–529.
19. Pavani S R P, Thompson M A, Bateen J S, et al. (2009) Three-dimensional, single-molecule fluorescence imaging beyond the diffraction limit by using a double-helix point spread function. *Proc. Natl Acad. Sci. USA* 106: 2995–2999.
20. Badieirostami M, Lew M D, Thompson M A, Moerner W E (2010) Three-dimensional localization precision of the double-helix point spread function versus astigmatism and biplane. *Appl. Phys. Lett.* 97: 161103.
21. Shtengel G, Galbraith J A, Galbraith C G, et al. (2009) Interferometric fluorescent super-resolution microscopy resolves 3D cellular ultrastructure. *Proc. Natl Acad. Sci. USA* 106: 3125–3130.
22. Aquino D, Schönle A, Geisler C, et al. (2011) Two-color nanoscopy of three-dimensional volumes by 4Pi detection of stochastically switched fluorophores. *Nat. Methods* 8: 353–359.
23. Xu K, Babcock H P, Zhuang X (2012) Dual-objective STORM reveals three-dimensional filament organization in the actin cytoskeleton. *Nat. Methods* 9: 185–188.
24. Jones S A, Shim S-H, He J, Zhuang X (2011) Fast, three-dimensional super-resolution imaging of live cells. *Nat. Methods* 8: 499–505.
25. Huang F, Hartwich T M P, Rivera-Molina F E, et al. (2013) Video-rate nanoscopy using sCMOS camera-specific single-molecule localization algorithms. *Nat. Methods* 10: 653–658.
26. Holden S J, Uphoff S, Kapanidis A N (2011) DAOSTORM: an algorithm for high-density super-resolution microscopy. *Nat. Methods* 8: 279–280.
27. Huang F, Schwartz S L, Byars J M, Lidke K A (2011) Simultaneous multiple-emitter fitting for single molecule super-resolution imaging. *Biomed. Opt. Express* 2: 1377–1393.
28. Zhu L, Zhang W, Elnatan D, Huang B (2012) Faster STORM using compressed sensing. *Nat. Methods* 9: 721–723.
29. Cox S, Rosten E, Monypenny J, et al. (2011) Bayesian localization microscopy reveals nanoscale podosome dynamics. *Nat. Methods* 9: 195–200.
30. Dertinger T, Colyer R, Iyer G, et al. (2009) Fast, background-free, 3D super-resolution optical fluctuation imaging (SOFI). *Proc. Natl Acad. Sci. USA* 106: 22287–22292.
31. Watanabe T M, Fukui S, Jin T, et al. (2010) Real-time nanoscopy by using blinking enhanced quantum dots. *Biophys. J.* 99: L50–L52.
32. Dempsey G T, Vaughan J C, Chen K H, et al. (2011) Evaluation of fluorophores for optimal performance in localization-based super-resolution imaging. *Nat. Methods* 8: 1027–1036.
33. Van de Linde S, Löschberger A, Klein T, et al. (2011) Direct stochastic optical reconstruction microscopy with standard fluorescent probes. *Nat. Protoc.* 6: 991–1009.
34. Xu K, Zhong G, Zhuang X (2013) Actin, spectrin, and associated proteins form a periodic cytoskeletal structure in axons. *Science* 339: 452–456.
35. Shim S-H, Xia C, Zhong G, et al. (2012) Super-resolution fluorescence imaging of organelles in live cells with photoswitchable membrane probes. *Proc. Natl Acad. Sci. USA* 109: 13978–13983.
36. Berk V, Fong J C N, Dempsey G T, et al. (2012) Molecular architecture and assembly principles of vibrio cholerae biofilms. *Science* 337: 236–239.
37. Bateen J S, Thompson M A, Tselenitis N K, et al. (2008) Super-resolution imaging in live Caulobacter crescentus cells using photoswitchable EYFP. *Nat. Methods* 5: 947–949.
38. Shroff H, Galbraith C G, Galbraith J A, Betzig E (2008) Live-cell photoactivated localization microscopy of nanoscale adhesion dynamics. *Nat. Methods* 5: 417–423.
39. Fölling J, Belov V, Kunetsky R, et al. (2007) Photochromic rhodamines provide nanoscopy with optical sectioning. *Angew. Chem. Int. Ed.* 46: 6266–6270.
40. Cella Zanacchi F, Lavagnino Z, Perrone Donnorso M, et al. (2011) Live-cell 3D super-resolution imaging in thick biological samples. *Nat. Methods* 8: 1047–1049.
41. Gustafsson M G (2000) Surpassing the lateral resolution limit by a factor of two using structured illumination microscopy. *J. Microsc.* 198: 82–87.
42. Lukosz W (1966) Optical systems with resolving powers exceeding the classical limit. *J. Opt. Soc. Am.* 56: 1463–1471.
43. Neil M A, Juskaitis R, Wilson T (1997) Method of obtaining optical sectioning by using structured light in a conventional microscope. *Opt. Lett.* 22: 1905–1907.
44. Gu M (2013) *Principles of Three-Dimensional Imaging in Confocal Microscopes* (World Scientific, Singapore).
45. Heintzmann R, Jovin T M, Cremer C (2002) Saturated patterned excitation microscopy – a concept for optical resolution improvement. *J. Opt. Soc. Am. A* 19: 1599–1609.
46. Gustafsson M G (2005) Nonlinear structured-illumination microscopy: wide-field fluorescence imaging with theoretically unlimited resolution. *Proc. Natl Acad. Sci. USA* 102: 13081–13086.
47. Rego E H, Shao L, Macklin J J, et al. (2012) Nonlinear structured-illumination microscopy with a photoswitchable protein reveals cellular structures at 50-nm resolution. *Proc. Natl Acad. Sci. USA* 109: E135–E143.
48. Gustafsson M G L, Shao L, Carlton P M, et al. (2008) Three-dimensional resolution doubling in wide-field fluorescence microscopy by structured illumination. *Biophys. J.* 94: 4957–4970.
49. Planchon T A, Gao L, Milkie D E, et al. (2011) Rapid three-dimensional isotropic imaging of living cells using Bessel beam plane illumination. *Nat. Methods* 8: 417–423.
50. Kner P, Chhun B B, Griffis E R, et al. (2009) Super-resolution video microscopy of live cells by structured illumination. *Nat. Methods* 6: 339–342.
51. Shao L, Kner P, Rego E H, Gustafsson M G L (2011) Super-resolution 3D microscopy of live whole cells using structured illumination. *Nat. Methods* 8: 1044–1046.

52. Fiolka R, Shao L, Rego E H, et al. (2012) Time-lapse two-color 3D imaging of live cells with doubled resolution using structured illumination. *Proc. Natl Acad. Sci. USA* 109: 5311–5315.
53. Schermelleh L, Carlton P M, Haase S, et al. (2008) Subdiffraction multicolor imaging of the nuclear periphery with 3d structured illumination microscopy. *Science* 320: 1332–1336.
54. Brown A C N, Oddos S, Dobbie I M, et al. (2011) Remodelling of cortical actin where lytic granules dock at natural killer cell immune synapses revealed by super-resolution microscopy. *PLoS Biol.* 9: e1001152.
55. Guizetti J, Schermelleh L, Mantler J, et al. (2011) Cortical constriction during abscission involves helices of ESCRT-III-dependent filaments. *Science* 331: 1616–1620.
56. Lawo S, Hasegan M, Gupta G D, Pelletier L (2012) Subdiffraction imaging of centrosomes reveals higher-order organizational features of pericentriolar material. *Nat. Cell Biol.* 14: 1148–1158.
57. Mennella V, Keszthelyi B, McDonald K L, et al. (2012) Subdiffraction-resolution fluorescence microscopy reveals a domain of the centrosome critical for pericentriolar material organization. *Nat. Cell Biol.* 14: 1159–1168.
58. Gao L, Shao L, Higgins C D, et al. (2012) Noninvasive imaging beyond the diffraction limit of 3d dynamics in thickly fluorescent specimens. *Cell* 151: 1370–1385.
59. Schmidt R, Wurm C A, Jakobs S, et al. (2008) Spherical nanosized focal spot unravels the interior of cells. *Nat. Methods.* 5: 539–544.
60. Westphal V, Rizzoli S O, Lauterbach M A, et al. (2008) Video-rate far-field optical nanoscopy dissects synaptic vesicle movement. *Science* 320: 246–249.
61. Bingen P, Reuss M, Engelhardt J, Hell S W (2011) Parallelized STED fluorescence nanoscopy. *Opt. Express* 19: 23716–23726.
62. Donnert G, Keller J, Medda R, et al. (2006) Macromolecular-scale resolution in biological fluorescence microscopy. *Proc. Natl Acad. Sci. USA* 103: 11440–11445.
63. Rittweger E, Han K Y, Irvine S E, Eggeling C, Hell S W (2009) STED microscopy reveals crystal colour centres with nanometric resolution. *Nat. Photonics* 3: 144–147.
64. Willig K I, Harke B, Medda R, Hell S W (2007) STED microscopy with continuous wave beams. *Nat. Methods* 4: 915–918.
65. Vicedomini G, Moneron G, Han K Y, et al. (2011) Sharper low-power STED nanoscopy by time gating. *Nat. Methods* 8: 571–573.
66. Hofmann M, Eggeling C, Jakobs S, Hell S W (2005) Breaking the diffraction barrier in fluorescence microscopy at low light intensities by using reversibly photoswitchable proteins. *Proc. Natl Acad. Sci. USA* 102: 17565–17569.
67. Grotjohann T, Testa I, Leutenegger M, et al. (2012) Diffraction-unlimited all-optical imaging and writing with a photochromic GFP. *Nature* 478: 204–208.
68. Hell S W, Kroug M (1995) Ground-state-depletion fluorescence microscopy: a concept for breaking the diffraction resolution limit. *Appl. Phys. B.* 60: 495–497.
69. Bretschneider S, Eggeling C, Hell S (2007) Breaking the diffraction barrier in fluorescence microscopy by optical shelving. *Phys. Rev. Lett.* 98: 218103.
70. Grotjohann T, Testa I, Reuss M, et al. (2012) rsEGFP2 enables fast RESOLFT nanoscopy of living cells. *eLife* 1: e00248.
71. Chmyrov A, Keller J, Grotjohann T, et al. (2013) Nanoscopy with more than 100,000 ‘doughnuts’. *Nat. Methods.* 10: 737–740.
72. Hein B, Willig K I, Hell S W (2008) Stimulated emission depletion (STED) nanoscopy of a fluorescent protein-labeled organelle inside a living cell. *Proc. Natl Acad. Sci. USA* 105: 14271–14276.
73. Jans D C, Wurm C A, Riedel D, et al. (2013) STED super-resolution microscopy reveals an array of MINOS clusters along human mitochondria. *Proc. Natl Acad. Sci. USA* 110: 8936–8941.
74. Tamarit B, Bugault F, Pillet A H, et al. (2013) Membrane micro-domains and cytoskeleton organization shape and regulate the IL-7 receptor signalosome in human cd4 t-cells. *J. Biol. Chem.* 288: 8691–8701.
75. Göttfert F, Wurm C A, Mueller V, et al. (2013) Coaligned dual-channel STED nanoscopy and molecular diffusion analysis at 20 nm resolution. *Biophys. J.* 105: L1–L3.
76. Maglione M, Sigrist S J (2013) Seeing the forest tree by tree: super-resolution light microscopy meets the neurosciences. *Nat. Neurosci.* 16: 790–797.
77. Willig K I, Rizzoli S O, Westphal V, et al. (2006) STED microscopy reveals that synaptotagmin remains clustered after synaptic vesicle exocytosis. *Nature* 440: 935–939.
78. Takasaki K T, Ding J B, Sabatini B L (2013) Live-cell superresolution imaging by pulsed STED two-photon excitation microscopy. *Biophys. J.* 104: 770–777.
79. Nägerl U V, Willig K I, Hein B, et al. (2008) Live-cell imaging of dendritic spines by STED microscopy. *Proc. Natl Acad. Sci. USA* 105: 18982–18987.
80. Urban N T, Willig K I, Hell S W, Nägerl U V (2011) STED nanoscopy of actin dynamics in synapses deep inside living brain slices. *Biophys. J.* 101: 1277–1284.
81. Eggeling C, Ringemann C, Medda R, et al. (2009) Direct observation of the nanoscale dynamics of membrane lipids in a living cell. *Nature* 457: 1159–1162.
82. Sieber J J, Willig K I, Kutzner C, et al. (2007) Anatomy and dynamics of a supramolecular membrane protein cluster. *Science* 317: 1072–1076.
83. Heller I, Sitters G, Broekmans O D, et al. (2013) STED nanoscopy combined with optical tweezers reveals protein dynamics on densely covered DNA. *Nat. Methods* 10: 910–916.
84. Enderlein J (2005) Breaking the diffraction limit with dynamic saturation optical microscopy. *Appl. Phys. Lett.* 87: 094105.
85. Fujita K, Kobayashi M, Kawano S, et al. (2007) High-resolution confocal microscopy by saturated excitation of fluorescence. *Phys. Rev. Lett.* 99: 228105.
86. Kawano S, Smith N I, Yamanaka M, et al. (2011) Determination of the expanded optical transfer function in saturated excitation imaging and high harmonic demodulation. *Appl. Phys. Express* 4: 042401.
87. Yamanaka M, Tzeng Y-K, Kawano S, et al. (2011) SAX microscopy with fluorescent nanodiamond probes for high-resolution fluorescence imaging. *Biomed. Opt. Express* 2: 1946–1954.
88. Yamanaka M, Saito K, Smith N I, et al. (2013) Saturated excitation of fluorescent proteins for subdiffraction-limited

- imaging of living cells in three dimensions. *Interface Focus* 3: 20130007.
89. Humpolickova J, Benda A, Enderlein J (2009) Optical saturation as a versatile tool to enhance resolution in confocal microscopy. *Biophys. J.* 97: 2623–2629.
90. Yamanaka M, Kawano S, Fujita K, et al. (2008) Beyond the diffraction-limit biological imaging by saturated excitation microscopy. *J. Biomed. Opt.* 13: 050507.
91. Yonemaru Y, Yamanaka M, Smith N I, et al. (2014) Saturated excitation microscopy with optimized excitation modulation. *Chem. Phys. Chem.* 15: 743–749.
92. Yamanaka M, Yonemaru Y, Kawano S, et al. (2013) Saturated excitation microscopy for sub-diffraction-limited imaging of cell clusters. *J. Biomed. Opt.* 18: 126002.
93. Hell S W (2007) Far-field optical nanoscopy. *Science* 316: 1153–1158.
94. Hell S W (2009) Microscopy and its focal switch. *Nat. Methods* 6: 24–32.
95. Requejo-Isidro J (2013) Fluorescence nanoscopy. Methods and applications. *J. Chem. Biol.* 6: 97–120.
96. Schermelleh L, Heintzmann R, Leonhardt H (2010) A guide to super-resolution fluorescence microscopy. *J. Cell Biol.* 190: 165–175.
97. Lau L, Lee Y L, Sahl S J, et al. (2012) STED microscopy with optimized labeling density reveals 9-fold arrangement of a centriole protein. *Biophys. J.* 102: 2926–2935.
98. Gould T J, Burke D, Bewersdorf J, Booth M J (2012) Adaptive optics enables 3D STED microscopy in aberrating specimens. *Opt. Express* 20: 20998–21009.
99. Lukinavičius G, Umezawa K, Olivier N, et al. (2013) A near-infrared fluorophore for live-cell super-resolution microscopy of cellular proteins. *Nat. Chem.* 5: 132–139.
100. Wang P, Slipchenko M N, Mitchell J, et al. (2013) Far-field imaging of non-fluorescent species with subdiffraction resolution. *Nat. Photonics* 7: 449–453.
101. Chu S-W, Su T-Y, Oketani R, et al. (2014) Measurement of a saturated emission of optical radiation from gold nanoparticles: application to an ultrahigh resolution microscope. *Phys. Rev. Lett.* 112: 017402.
102. Chu S-W, Wu H-Y, Huang Y-T, et al. (2014) Saturation and reverse saturation of scattering in a single plasmonic nanoparticle. *ACS Photonics* 1: 32–37.
103. Beeker W P, Lee C J, Boller K J, Groß P, Cleff C, Fallnich C, Offerhaus H L, Herek J L. (2011) A theoretical investigation of super-resolution CARS imaging via coherent and incoherent saturation of transitions. *J. Raman Spectrosc.* 42: 1854–1858.
104. Kogure S, Inoue K, Ohmori T, Ishihara M, Kukuchi M, Fujii M, Sakai M. (2010) Infrared imaging of an A549 cultured cell by a vibrational sum-frequency generation detected infrared super-resolution microscope. *Opt. Express* 18: 13402–13406.